Advanced oxidation processes for removal of monocyclic aromatic hydrocarbon from water: Effects of O_3/H_2O_2 and UV/H_2O_2 treatment on product formation and biological post-treatment

*Emil Bein[a], Bettina Seiwert[b], Thorsten Reemtsma[b], Jörg E. Drewes[a] and Uwe Hübner[a]**

[a] Chair of Urban Water Systems Engineering, Technical University of Munich, Am Coulombwall 3, 85748 Garching, Germany

[b] Department of Analytical Chemistry, Helmholtz Centre for Environmental Research – UFZ, Permoserstrasse 15, 04318 Leipzig, Germany

* Corresponding author: u.huebner@tum.de (U. Hübner)

Keywords

Advanced oxidation processes; monocyclic aromatic carbon; reaction kinetics; ozone; hydroxyl radicals.

Graphical abstract

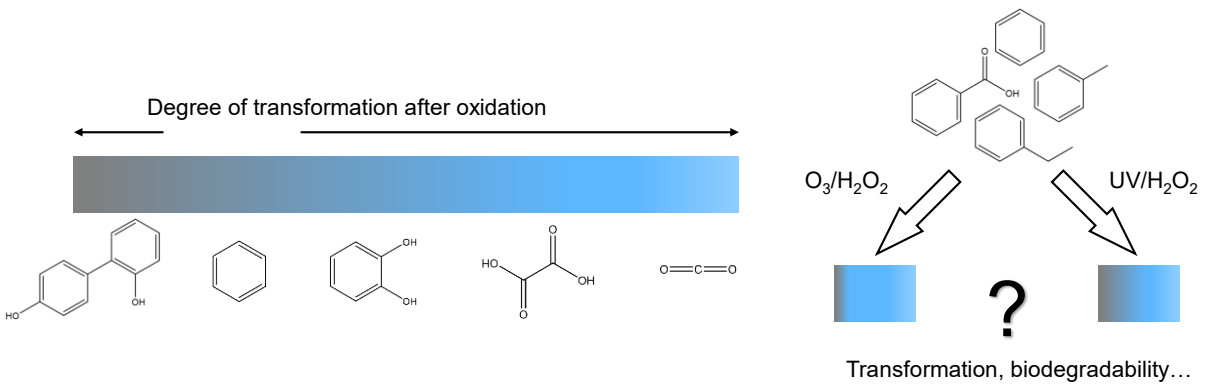

Abstract

Several oxidative treatment technologies, such as ozonation or Fenton reaction, have been studied and applied to remove monocyclic hydroaromatic carbon from water. Despite decades of application, little seems to be known about formation of transformation products while employing different ozone- or ˙OH-based treatment methods and their fate in biodegradation. In this study, we

demonstrate that O_3/H_2O_2 treatment of benzene, toluene, ethylbenzene (BTE), and benzoic acid (BA) leads to less hydroxylated aromatic transformation products compared to UV/H_2O_2 as reference system – this at a similar $^{\cdot}OH$ exposure and parent compound removal efficiency. Aerobic biodegradation tests after oxidation of 0.15 mM BA (12.6 mg C L^{-1} theoretical DOC) revealed that a less biodegradable DOC fraction >4 mg C L^{-1} was formed in both oxidative treatments compared to the BA control. No advantage of ozonation over UV/H_2O_2 treatment was observed in terms of mineralization capabilities, however, we detected less transformation products after oxidation and biodegradation using high-resolution mass spectrometry. Biodegradation of BA that was not oxidized was more complete with minimal organic residual. Overall, the study provides new insights into the oxidation of monocyclic aromatics and raises questions regarding the biodegradability of oxidation products, which is relevant for several treatment applications.

1 Introduction

Monocyclic aromatic hydrocarbons, most importantly BTEX (benzene, toluene, ethylbenzene, o-, p-, and m-xylene), are abundant, toxic groundwater contaminants that show high resistivity towards powerful oxidants such as ozone due to their aromatic ring without activating group (Hoigné and Bader, 1983; von Sonntag and von Gunten, 2012). Various AOPs have been proposed in the past to achieve an efficient removal of BTEX compounds from contaminated water (Bustillo-Lecompte et al., 2018; Dutschke et al., 2022; Fernandes et al., 2019a; Fernandes et al., 2019b; Garoma et al., 2008; Kasprzyk-Hordern et al., 2005; Rayaroth et al., 2023; Yang et al., 2020). For *in-situ* treatment of BTEX contamination, ozonation by sparging gas into wells is a state-of-the-art field-scale groundwater remediation technology (Krembs et al., 2010; Nimmer et al., 2000; Siegrist et al., 2011). Due to the low direct reactivity of BTEX with ozone, oxidation efficiency relies on the *in-situ* generation of $^{\cdot}OH$ from the reaction of ozone with the soil matrix or simultaneously injected hydrogen peroxide. Depending on the concentration, self-enhanced removal may occur due to radicals produced by reactions of hydroxylated intermediates with ozone, as it has been shown for benzoic acid (BA) (Huang et al., 2015).

Important criteria to study the efficacy of oxidative treatment are the enhanced removal of target contaminants compared to other tested treatment methods, but also the required energy input

(Katsoyiannis et al., 2011; Miklos et al., 2019; Sgroi et al., 2021). However, complete mineralization is extremely energy-intense and rarely achieved in oxidative treatment and, hence, the formation of transformation products (TPs) appears unavoidable. Therefore, ozonation – which is a very established process in advanced water treatment – is often coupled with biological post-treatment for lowering DOC and removing TPs of micropollutants in treated effluent (Itzel et al., 2020; Schollée et al., 2018). Generally, energy reductions are also postulated for coupling of other AOPs, such as electrochemical Fenton and Photo-Fenton processes, with biological post-treatment due to the suspected formation of more readily biodegradable intermediates (Huang et al., 2017; Oller et al., 2011). Biodegradability of intermediates is also relevant for *in-situ* groundwater remediation, as mineralization of remaining organic carbon is desired but difficult to achieve with chemical oxidation only, requiring coupling strategies of biological and chemical treatment (Sutton et al., 2011).

In this study, we investigate the transformation of monocyclic aromatics, namely benzene, toluene, ethylbenzene (BTE) and benzoic acid (BA) during O_3/H_2O_2 and UV/H_2O_2 treatment. These target contaminants have been proven prone to $^{\cdot}OH$ attack with reported second-order rate constants $>10^9 M^{-1} s^{-1}$ (Buxton et al., 1988), leading to hydroxylated (i.e., phenolic) TPs: For instance, phenol and o-, p- and m-cresol have been reported as TPs in different UV-based AOPs (UV/NO_3^- and UV/TiO_2) of benzene and toluene as result of H-abstraction reactions (Hatipoglu et al., 2010; Park and Choi, 2005). For toluene and ethylbenzene, other aromatic structures resulting from $^{\cdot}OH$ attack (H-abstraction) at the methyl and ethyl group were detected (Cui et al., 2017; Hatipoglu et al., 2010).

We hypothesize that an oxidation process including both, ozone and $^{\cdot}OH$ production, will have synergistic effects for treating monocyclic aromatic hydrocarbons based on known reaction pathways of hydroxylated intermediates. Phenol, the major product of benzene oxidation with $^{\cdot}OH$ (Park and Choi, 2005), is highly reactive with ozone (supplemental information (SI), Figure S5, Table S1). It can be directly transformed to aliphatic acids such as cis,cis-muconic acid by ring-cleavage or to other intermediates with intact ring structure, for instance catechol and p-benzoquinone (Mvula and von Sonntag, 2003; Ramseier and von Gunten, 2009). All of these compounds are further reacting with ozone, eventually giving rise to small products with low ozone reactivity such as oxalic and formic acid. Similar mechanisms and reactivities are expected for toluene, ethylbenzene and BA due to their

structural similarity and the formation of hydroxylated products that are reactive with ozone. A different composition of intermediates can be expected in AOPs with $^{\cdot}OH$ as major oxidant (such as UV/H_2O_2) due to the absence of ozone. This rapid breakdown of monocyclic aromatic compounds to aliphatic products in ozone-based AOPs is expected to enhance aerobic biodegradation and mineralization of oxidation TPs by microbial communities in the aquifer.

The aim of this investigation is to determine differences of O_3/H_2O_2 ("peroxone") and UV/H_2O_2 AOPs for transformation of mostly ozone- and photo-resistant monocyclic aromatic hydrocarbons. We also study the effect of different oxidative treatments on subsequent biodegradation of dissolved organic matter for BA. Due to assumed similarities of BA and BTE, BA may serve as good model compound for biological post-treatment as it is non-volatile and therefore more suitable to assess the degree of mineralization.

2 Materials and methods

2.1 Chemicals and reagents

The purity of all quantified organic compounds was higher than 98%. Used chemicals are listed in the SI, Table S2. Experimental solutions for BTE experiments were freshly prepared by directly diluting BTE into pH 7 phosphate buffer solution (PBS) with a final concentration of 10 mM on the days of experiments. Concentrated PBS (0.5 M) was prepared with $NaH_2PO_4 \cdot 2H_2O$ and Na_2HPO_4 in ultrapure water (UPW). The final pH was then adjusted by adding either phosphoric acid or sodium hydroxide. 20 mM H_2O_2 stock solutions were freshly prepared from 30% stabilized H_2O_2 (VWR Chemicals) on each day and added accordingly.

2.2 Oxidation experiments

2.2.1 O_3/H_2O_2 process for BTE treatment

BTE were oxidized in closed recirculation experiments using a gas-liquid membrane contactor in counter-current flow for O_3/H_2O_2 treatment (Figure 1a). Experimental set-ups are designed to allow direct comparisons of BTE removal during both AOPs as function of $^{\cdot}OH$ exposures by avoiding losses

due to volatilization. They are not intended to optimize the treatment efficiency, neither with respect to treatment time nor oxidant dose. All materials in contact with the solution were made of PTFE, PVDF, PEEK, glass, or stainless steel.

The ozone membrane contacting unit consisted of a glass column with 22 cm inner diameter that was equipped with gas-tight in- and outlets for gas- and liquid-streams (Bühler Technologies GmbH, Germany). Porous PTFE (FluorTex GmbH, Germany) was chosen as membrane material due to its high ozone-resistance and mass transfer (Bein et al., 2021). The 25.5 cm membrane tube was installed inside the glass column and had an inner diameter of 2.8 mm, a wall thickness of 0.5 mm, and a porosity of 50%. Ozone gas with a concentration of 200 g Nm^{-3} was generated by a BMT 803 BT ozone generator, analyzed by a BMT 964 analyzer (BMT Messtechnik GmbH, Germany) and inserted at a flow rate of approximately 0.25 NL min^{-1} from top to bottom of the glass column. The liquid was pumped from bottom to top through the membrane tube (Figure 1a, counter-current configuration). A needle valve was used to control liquid-side pressure to achieve bubble-free ozonation, where ozone directly diffuses into the gas-liquid boundary layer in proximity to the membrane surface (Bein et al., 2021).

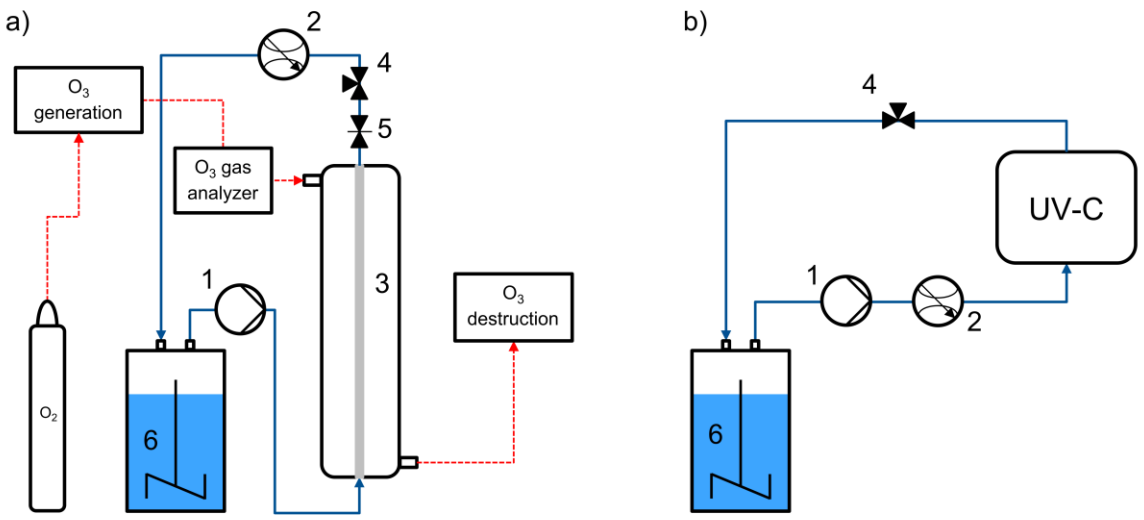

Figure 1: Experimental set-ups for recirculation experiments: a) ozone membrane contacting, b) UV-C irradiation. 1: gear pump, 2: flow meter, 3: PTFE membrane, 4: sampling port, 5: needle valve, 6: stirred feed solution.

For every ozone membrane contacting experiment, a 0.6 L solution was prepared containing 10 mM PBS (pH 7), 0.1 µM pCBA, 30 mg L^{-1} H_2O_2 (0.88 mM) and BTE (0.12-0.25 mM). BTE

concentrations varied considerably among experiments due to the applied procedure to prepare solution, which is discussed in section 3. The solution was transferred to a closed glass bottle of the same volume to keep the gas-liquid contact area and volatility losses low. The constantly stirred solution was pumped through the recirculation set-up at a flow rate of 6.5 L h^{-1} that was controlled by a DK 800 Krohne rotameter (Krohne Messtechnik GmbH, Germany). This corresponds to approximately 0.3 m s^{-1} liquid flow velocity in the membrane and a theoretical ozone mass transfer coefficient of $1.77 \cdot 10^{-5}$ m s^{-1} (Lévêque solution, without chemical reaction). 20 mL samples plus 20 mL sample port flush were withdrawn from a three-way valve after different recirculated volumes. The time after one volume recirculated was defined as volume of the solution divided by the liquid flow rate. Sampling times were corrected for volume removed accordingly. The first 20 mL sample was taken from the bottle prior to start. 9.4 mL of sample were filled immediately into headspace (HS) vials, prepared for GC-FID analysis according to the analytical method, and quickly sealed to avoid further losses. An aliquot of the sample was directly analyzed for UV/Vis absorbance. The remainder was quenched with 1 mM $Na_2S_2O_3$ to remove any remaining O_3 or H_2O_2 pending further analysis.

2.2.2 UV/H_2O_2 process for BTE treatment

UV/H_2O_2 treatment and sampling was performed analogously using a UV-C flow-through reactor with the same water matrix as in ozonation experiments with 1.1 L feed solution at a flow rate of 10 L h^{-1} (Figure 1b). Additionally, photo-resistant probe compounds carbamazepine (CBZ), gabapentin (GBP) and primidone (PRI) were added at trace concentrations of 0.05 (CBZ) and 0.1 µM (GBP, PRI) instead of pCBA (Miklos et al., 2018). pCBA could not be used as probe compound in UV-based treatment due to its decay in a control experiment without H_2O_2. A discussion on the probe compound selection can be found in the SI, Text S1. UV-C light was emitted using a 10W LP mercury lamp in a stainless-steel flow-through system (Purion GmbH, Germany) with an irradiated reactor volume of approximately 105 mL.

2.2.3 Oxidative treatment of BA

Oxidation of 0.15 mM BA prior to biodegradation experiments was conducted in diluted natural water instead of PBS. Tap water (TW) of an approximate pH of 7.7 and DOC < 1 mg C L^{-1} was chosen

as natural buffer system and diluted with UPW at a ratio of 1:2.85 TW:UPW to achieve the same water matrix for all samples during ozonation and UV/H_2O_2 treatment. For UV/H_2O_2 experiments, the UV-C set-up described in 2.2.2 was used. Sample volumes were increased to 200 mL (plus 20 mL sample port flush) with a total recirculation volume of 1.5 L. Withdrawn samples were also quenched with 1 mM $Na_2S_2O_3$ and stored at -20 °C after taking samples for BA and TOC until subsequent biodegradation experiments. TOC samples were acidified with two droplets 32% HCl (≤ pH 2) and stored at 4°C prior to analysis.

As BA is non-volatile, O_3/H_2O_2 treatment was performed in batch experiments with addition of pre-defined amounts of ozone stock solution and H_2O_2 in a molar ratio of 2:1 followed by short stirring (<1 min). Ozone stock solutions of approximately 52 mg L^{-1} were produced with the ozone generator described in section 2.2.1 in a cooled (4 °C) 2.5 L glass reactor with a porous bubble diffusor that was constantly supplied with gaseous ozone. The applied ozone doses ranged from 0.1 to 0.7 mM. $^{\cdot}OH$ exposure in O_3/H_2O_2 batch experiments was determined using PRI instead of pCBA that also agreed closely with UV/H_2O_2 data.

2.3 Aerobic biodegradation experiments

Initial biodegradation was assessed in batch experiments by inoculating 60 mL samples with 10 g sand (wet weight) from the top layer of a biological sand filtration column, continuously fed with aerated wastewater treatment plant effluent from top to bottom for more than 6 weeks before experiments. The sand was homogenized and carefully washed with TW on a 200 µm stainless steel sieve to remove remaining wastewater. Inoculated batches (250 mL amber glass bottles) were closed with perforated lids, shaken at 125 rpm for 6 days, and 6 mL samples for DOC analysis were taken several times. Oxic conditions (> 7 mg L^{-1} dissolved oxygen) were confirmed by daily measurements using flow-through cells, where sample was pumped through using a plastic syringe (FTC-PSt3, Presens, Germany). For abiotic control experiments, three times 10 g biologically active sand was placed in amber bottles for shake tests and autoclaved to demonstrate inhibited biological activity.

Samples for DOC analysis were immediately filtered through 0.45 µm cellulose acetate filters that were pre-rinsed with 200 mL UPW and approximately 0.5 mL of sample. Samples were diluted

with UPW (DF 0.167) and acidified as for TOC analysis. Biodegradation tests were performed in triplicates for each sample taken from oxidation experiments. The selected samples for biodegradation experiments are specified in section 0 and Text S2 (SI).

2.4 Analytical methods

BTE were measured by an Agilent 7980 GC gas chromatograph with headspace auto-sampling module coupled with flame ionization detection (HS-GC/FID). Compound separation was performed on a 30 m column with 0.32 mm inner diameter and 1.80 µm film thickness (DB-624, Agilent, USA), using nitrogen as carrier gas. The initial oven temperature of 40 °C was kept for 3 min and increased by 12.5 °C min^{-1} to 250 °C. Detailed instrument settings are listed in the SI, Table S3. Calibration standards (1-50 mg L^{-1}) were prepared from a BTE stock solution in MeOH, which was added to headspace vials, filled up to 0.6 mL MeOH and mixed with 9.5 mL UPW and 0.5 g sodium sulfate. Accordingly, 9.4 mL samples + 0.1 mL UPW were mixed with 0.6 mL MeOH instead of the calibration standard, and the same amount of salt was added.

BTE TPs and BA were analyzed using an Agilent 1260 Infinity II high performance liquid chromatography system with diode array detector (HPLC-DAD). Two separate methods were applied: phenol, o-cresol and o-ethylphenol (0.1-5 mg L^{-1}) were separated on an XSelect HSS C18 column (2.1 x 100 mm, 3.5 µm particle size) at a flow rate of 0.5 mL min^{-1}, using a gradient method with H_2O and acetonitrile (ACN) as solvents. All of the three compounds were detected at 275 nm. Wavelength scans were performed in parallel to confirm the compounds via retention time and spectrum. BA (0.25-10 mg L^{-1}) was detected using the same system but at a flow rate of 0.6 mL/min (0.1% formic acid in H_2O and ACN), at 238 nm. The injection volume was 50 µL for both methods. Further details are listed in the SI, Table S4.

Quantitation of $^{\cdot}OH$ probe compound candidates PRI, CBZ, GBP was performed with an LC-MS/MS system in scheduled MRM mode (positive ESI) using isotope labelled standard (IS) correction (0.0025 – 10 µg/L). The system is composed of a SCIEX Triple Quad 6500 mass spectrometer (SCIEX, USA) coupled with a Knauer PLATINBLUE UHPLC (Knauer, Germany) and an XSelect HSS T3 (particle size 2.5 µm; 2.1 x 100 mm) column (Waters, USA). More details on the method can be found

in Müller et al. (2017). pCBA (m/z 111) was analyzed similarly with internal standard correction (pCBA d4) in negative ESI mode with 0.1% acetic acid in H_2O and ACN as solvents and a modified gradient.

TOC/DOC (0.1-10 mg C L^{-1}) was analyzed on a VarioTOC TOC/DOC analyzer (Elementar, Germany). Organic carbon in chemical oxidation experiments was determined as TOC (analysis without filtration) and in biodegradation experiments as DOC. However, no noteworthy differences between TOC and DOC became apparent in pre-tests, thus we assumed TOC≈DOC. UV spectra were recorded using a Hach DR6000 UV/Vis spectrophotometer (200-800 nm). Excitation emission matrices (EEMs) were obtained by an Aqualog (HORIBA Jobin Yvon, Germany). EEM samples were filtered as for DOC analysis and diluted 1:13. Obtained EEM data was modified including corrections for inner filter effects, Rayleigh masking, and Raman normalization (Bahram et al., 2006).

An identification of chemical structures of oxidation products in BA experiments was undertaken using RPLC-HRMS screening, following the method described by Seiwert et al. (2021). Briefly, screenings were performed with an ACQUITY UPLC system connected to a XEVO G2 XS TOF MS equipped with an electrospray ionization source (Waters, USA). In addition, a fluorescence detector was connected and set to regions identified in EEMs (290/410 nm and 320/450 nm). Contrary to Seiwert et al. (2021), ACN was used as solvent B instead of MeOH. All relevant compounds were identified in negative ESI. Sum formulas of peaks were identified based on exact mass and structures proposed where applicable. Further details can be found in the SI, Table S5.

3 Results

3.1 Removal kinetics during O_3/H_2O_2 and UV/H_2O_2 treatment

Oxidative treatment of BTE in neutral PBS led to similar partial removal of all three contaminants (Figure S6). By the end of the treatment, between 60 and 70% of BTE were removed in both processes. To achieve this removal in the ozone membrane contactor, the treated solution was circulated 50 times, compared to 5 times during UV/H_2O_2 treatment. This is a consequence of the comparably small ozone dose transferred in the short (25.5 cm) single tube contactor if compared to

larger hollow fiber membrane modules used in some previous works (Leiknes et al., 2005; Zhang et al., 2017).

Removal of ozone- and UV-resistant probe compounds was used to determine $^{\cdot}OH$ exposures during O_3/H_2O_2 and UV/H_2O_2 treatment and compare both oxidative treatments on the basis of similar $^{\cdot}OH$ exposures (Figure 2). The $^{\cdot}OH$ exposure values were calculated using second-order reaction rate kinetics with reported rate constants of probe compounds, as discussed previously (e.g., Rosenfeldt et al. (2006) and Wünsch et al. (2021)). The final selection of two probe compounds (CBZ for UV/H_2O_2 and pCBA for O_3/H_2O_2) resulted in good agreement of contaminant removal kinetics for both, BTE and BA experiments with a more pronounced deviation of the two treatment processes in case of BA experiments (SI, Text S1). Data point scattering in BTE experiments was observed for all three compounds and is most likely related to sampling and analysis of the volatile substances. PRI with a reported rate constant of $6.7 \cdot 10^9$ M^{-1} s^{-1} (Real et al., 2009) led to similar results as pCBA for BA ozonation experiments, confirming that both are suitable probe compounds for measuring $^{\cdot}OH$ exposure during ozonation (Figure 5).

For further validation, second-order rate constants were determined from the slope of the linear fit of O_3/H_2O_2 data points in Figure 2a and b as $7.7 \cdot 10^9$ $M^{-1}s^{-1}$ for benzene ($7.4 \cdot 10^9$ $M^{-1}s^{-1}$ for UV/H_2O_2) and $5.6 \cdot 10^9$ $M^{-1}s^{-1}$ for BA ($6.3 \cdot 10^9$ $M^{-1}s^{-1}$ for UV/H_2O_2), respectively. These values are in close agreement with previously reported respective values of $7.8 \cdot 10^9$ M^{-1} s^{-1} (Schuler and Albarran, 2002) and $5.9 \cdot 10^9$ M^{-1} s^{-1} (Buxton et al., 1988). Rate constants of toluene and ethylbenzene are very similar to that of benzene (SI, Figure S7). These results confirm the plausibility of calculated $^{\cdot}OH$ exposures. Moreover, they indicate that $^{\cdot}OH$ oxidation is the major removal mechanism for BTE, and volatilization, ozonolysis, or photolysis were insignificant.

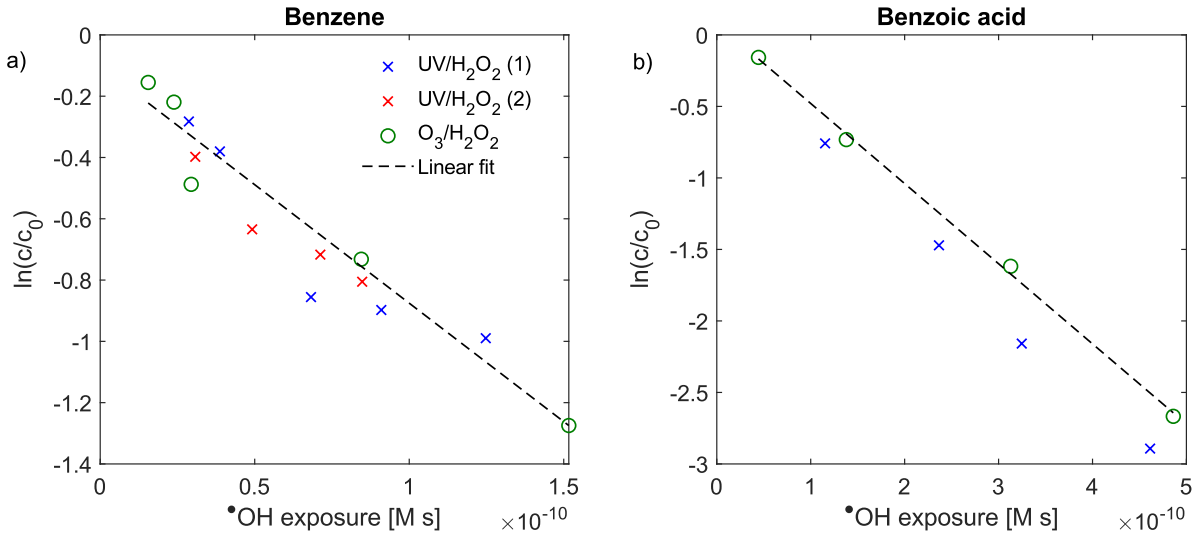

Figure 2: Removal of (a) benzene during BTE oxidation experiments and (b) BA during separate experiments as function of ˙OH exposure. Displayed linear fits were calculated with O_3/H_2O_2 data points. The shown UV/H_2O_2 experiment with BA was performed in diluted TW instead of PBS.

3.2 Product formation during BTE oxidation

3.2.1 Hydroxylated transformation products

HPLC-DAD analysis of treated samples confirmed a constant formation of the hydroxylated TPs phenol, o-cresol and o-ethylphenol in UV/H_2O_2 treatment (Figure 3). Interestingly, the observed yield of o-ethylphenol from ethylbenzene (20.6 ± 2.6%) was much higher than of phenol (2.2 ± 1.0%) and o-cresol (4.1 ± 0.6%) from benzene and toluene, respectively. In contrast, none of the three compounds were found in samples treated with O_3/H_2O_2 (lowest point of calibration 0.0011-0.0.00082 mM or 0.1 mg L^{-1}), likely due to direct reaction with ozone present at the boundary layer of the ozone membrane contactor, where compounds such as phenol are quickly oxidized via electron transfer and formation of ozone adduct intermediates (Ramseier and von Gunten, 2009). This also indicates that enough ozone was available to directly oxidize intermediates, while simultaneous ˙OH production occurs through reactions with H_2O_2 (Merényi et al., 2010) and potentially through the reactions with phenolic intermediates (Huang et al., 2015). Contrarily, formation rates of these TPs in UV/H_2O_2 treatment must be higher than any subsequent decay, either by radicals or photolysis, as long as BTE are still present in larger amounts, which was the case in all experiments. Direct photolysis of intermediates and resulting production of other reactive oxygen species during UV-irradiation cannot be excluded, but has been reported for phenol only for much longer exposure times of several hours or substantially stronger UV-

lamps (e.g., 500 W), and can therefore only be a minor contribution in the experimental conditions of the study (Alapi and Dombi, 2007; Chun et al., 2000).

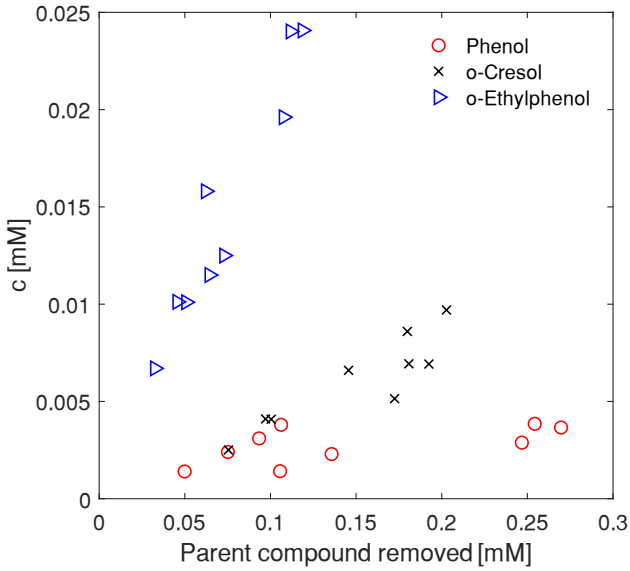

Figure 3: Concentration of hydroxylated TPs over the course of UV/H_2O_2 treatment. Parent compounds: benzene (phenol), toluene (o-cresol), ethylbenzene (o-ethylphenol).

The formation of hydroxylated TPs in the ˙OH-based process is in accordance with previous literature findings. The yield of o-cresol during photochemical oxidation of 1.4 mM toluene reported by Hatipoglu et al. (2010) was 30.5% and 77.5% for all cresol isomers. Less than 10% of initial toluene was transformed in this experiment, which may explain the comparably high yield and the absence of other TPs. Cui et al. (2017) degraded 1 mM ethylbenzene using a modified Fenton reaction, where ˙OH was demonstrated to be the main reactant by scavenger control experiments. Besides o-, m- and p-ethylphenol, they also found acetophenone and β-phenylethanol as TPs, suggesting that ˙OH may also abstract hydrogen at the ethyl moiety with subsequent oxygen attachment. A corresponding reaction with toluene may lead to benzaldehyde or BA. These compounds were not addressed analytically in this experiment though. The absence or low quantity of the analyzed hydroxylated TPs in O_3/H_2O_2 treatment demonstrates the effect of ozone exposure, leading to immediate transformation of hydroxylated TPs of BTE.

3.2.2 Change of Absorbance

UV/vis absorbance spectra were recorded to check for formation of absorbance peaks characteristic for different types of organic carbon with conjugated π-electron systems. Absorbance increased during both treatments in the UV range (Figure 4a, Figure S8). This differs from wastewater ozonation, where UV-absorbance is reduced while conjugated π-electron systems in aromatic and olefinic compounds are decomposed by ring-cleavage and the Criegee mechanism (Criegee, 1975; Lamsal et al., 2011; Nöthe et al., 2009; Wenk et al., 2013). Indeed, a stronger increase was observed for UV/H_2O_2 treatment with two pronounced peaks at 275 and 350 nm that were absent during O_3/H_2O_2 treatment. This is highlighted by changes of absorbance at selected wavelengths (275 nm/350 nm, Figure 4b and c versus $^{\bullet}$OH exposures. Although initial concentrations were different, the qualitative comparison shows that larger wavelengths are only absorbed in the samples treated with UV/H_2O_2, which also resulted in visible color formation. Similar differences between the two treatments were also observed for BA (Figure S9, SI).

The stronger absorbance increase of samples treated with UV/H_2O_2 at 275 nm (Figure 4b) is attributed to hydroxylated or di-hydroxylated compounds that show maximum absorbance at 260-280 nm and are abundant in these samples (see section 3.2.1). At the end of UV/H_2O_2 treatment, an absorbance of 0.786 was measured compared to only 0.176 in case of O_3/H_2O_2. As single-hydroxylated TPs were not detected in case of O_3/H_2O_2, the observed rise is either caused by lower concentrations or the absorbance of other compounds.

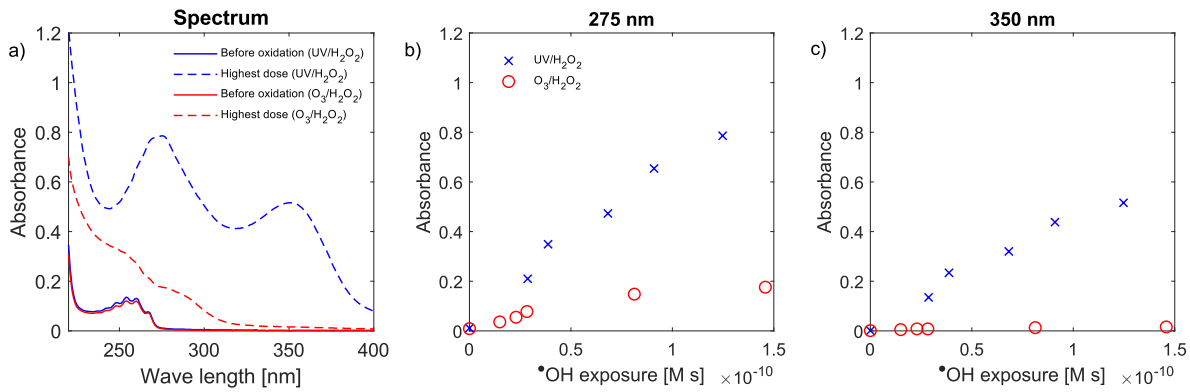

Figure 4: Absorbance change over the whole spectrum during oxidative treatment (a), and for selected wavelengths as a function of $^{\bullet}$OH exposure (b,c). Initial BTE concentrations were 0.43/0.28/0.18 mM (UV/H_2O_2) and 0.25/0.25/0.12 mM (O_3/H_2O_2) (see also Tables S6-S10).

The other distinct absorbance increase during UV/H_2O_2 treatment for larger wavelengths, most notably at 350 nm (Figure 4c), may occur by formation of a large diversity of other hydroxylated aromatic or other structures with intact π-electron systems, for example p-benzoquinone, which also absorbs strongly between 300 and 500 nm (Nagakura and Kuboyama, 1954). Due to its fast reaction with ozone (Table S1, SI), the absence in the respective spectrum would be plausible. Another possibility is the highly concentration-dependent polymerization of aromatic rings that has been observed for phenol during pulsed radiolysis at a much higher concentration of 0.02 M (1.88 g L^{-1}) (Ye and Schuler, 1989). A similar reaction is described for aniline at a concentration of 150 mg L^{-1} (Shang and Yu, 2002). The potential for the formation of such dimers or even polymers will be discussed further in section 0 for BA.

3.3 Coupling chemical oxidation and biodegradation

3.3.1 O_3/H_2O_2 and UV/H_2O_2 treatment of BA

Oxidative treatment resulted in reduction of BA concentration up to 94% depending on the $^{\cdot}OH$ exposure, but only minor mineralization, expressed as reduction of TOC (Figure 5a). TOC decreased by approximately 2.6 mg C L^{-1} in both processes by applying the highest doses. Initial BA concentrations were very similar (17.85 and 17.16 mg L^{-1}), but initial TOC was slightly elevated in UV/H_2O_2 treatment (ca. + 2 mg C L^{-1}). The initial BA concentration (17.85 mg L^{-1}) in the O_3/H_2O_2 control sample corresponds to a theoretical TOC of 12.3 mg C L^{-1}, which is in good agreement with the measured TOC of 13 mg C L^{-1} confirming that BA is the major organic carbon source in the samples with only minor contributions of natural organic matter in the used TW.

UV/vis spectra were recorded for each oxidative step (Figure S9, SI). Analogously to BTE oxidation, an increase of absorbance was observed for both, UV/H_2O_2 and O_3/H_2O_2 treatment of BA. Color formation occurred, also indicated by absorbance increases for 400 nm and larger. Interestingly, colorization was more apparent during ozonation of BA as for BTE. Such color formation, expressed as increased absorption at 420 nm during ozonation of BA, was already reported by Shang and Yu (2002), who did not further elaborate the formation of individual TPs. However, they detected increased toxicity for low ozone doses.

3.3.2 Aerobic microbial degradation

Samples highlighted with number codes in Figure 5a were used for biodegradation experiments in triplicates (Figure 5b). Oxidized samples (1a and 1b) exhibited a strong reduction of DOC after two days. However, biodegradation stopped after approximately three days and the DOC content remained above 4 mg L^{-1} until day 6. Contrarily, DOC present in the BA sample not treated with oxidants (0a) was removed to concentrations below 2 mg L^{-1} after 6 days (Figure 5b). Similar results were observed in replicate experiments with samples (0b), (1b) and (2a) (Figure S8, SI). Only after five days a minor reduction of DOC could be observed in control experiments with autoclaved sand, which may be related to regrowth of bacteria as experiments were not conducted under sterile conditions. It demonstrates that removal of DOC in the first three days of biodegradation tests was not related to sorption effects (Figure 5b). Differences between UV/H_2O_2 and O_3/H_2O_2 treatment were small and did not support the hypothesis that the ozone-based AOP improves rapid biodegradation compared to the UV-based AOP of BA.

The reduced biodegradability of the DOC after oxidation contradicts previous studies on ozonation of treated wastewater with subsequent biological post-treatment (Hübner et al., 2012). It indicates that overall biodegradability of TPs should be considered in more detail, especially when combining AOPs with biological treatment for industrial or groundwater applications, where only a few contaminants may dominate the organic water constituents. For instance, Pariente et al. (2008) concluded that photo-Fenton oxidation improved aerobic biodegradability of treated BA (150 mg L^{-1}), expressed as faster reduction of COD in biological shake flask tests after oxidation compared to untreated BA. However, sum parameters such as COD or BOD_5 might have a limited meaning, as they do not fully indicate, if refractory compounds have been formed. Additionally, they continued oxidative treatment after BA was fully removed, which may improve biodegradability but is also energy intensive.

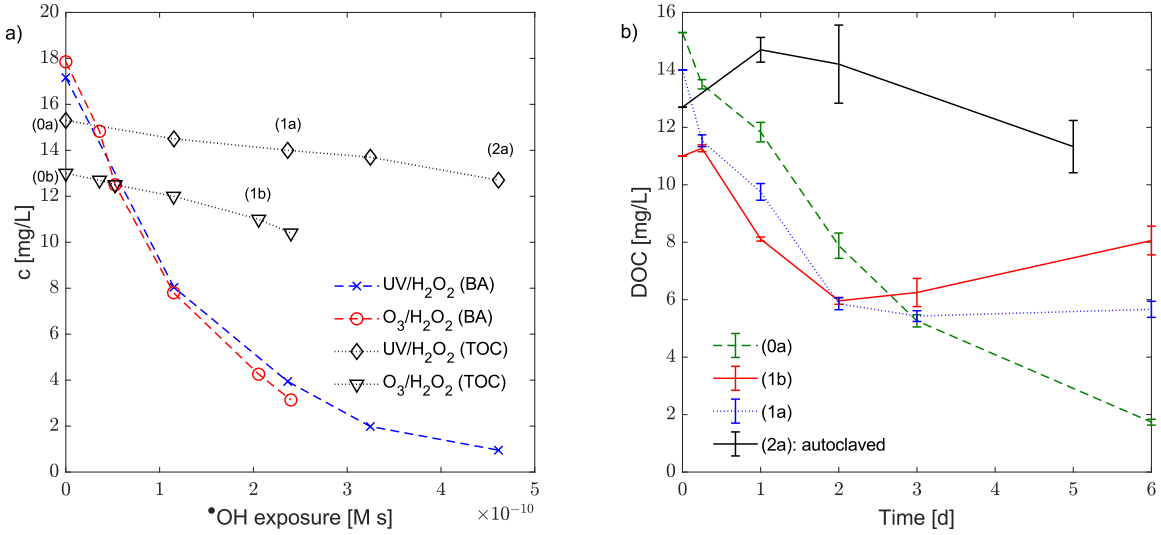

Figure 5: Chemical oxidation of BA and subsequent biodegradation. a) changes of BA concentrations and TOC vs. ˙OH radical exposure. b) Degradation of DOC in shaken batches of selected samples withdrawn in oxidation experiments. Standard deviations originate from DOC data of three individual batches containing the same water matrix (n=3). TOC from a) was taken as initial value. The shaker was temporarily interrupted on day 5-6 (samples 0a and 1a) with dissolved oxygen levels staying well above 7 mg L^{-1} during that time. Data of more batches is visualized in Figure S4.

3.3.3 Analysis of transformation products after oxidation and after biodegradation

In order to investigate refractory compounds after biodegradation, excitation emission matrices (EEMs) were recorded before and after oxidation, and after biodegradation. UV/H_2O_2 treatment led to a substantial increase in fluorescence with two maximum regions at approximately 290/410 nm (peak 1) and 320/450 nm (peak 2) (Figure 6). Peak 1 is very similar to what has been reported previously for o-hydroxybenzoic acid (salicylic acid) (Ni et al., 2006). After biodegradation a weaker signal (22-24 Raman units before, 6-7 after) could be found for the latter peak, which indicates that larger, fluorescing molecules remained present to some degree as refractory DOC. The same can be observed for O_3/H_2O_2, where only peak 2 (320/450 nm) was formed and also remained present with weaker intensity after biodegradation (Figure S10, SI).

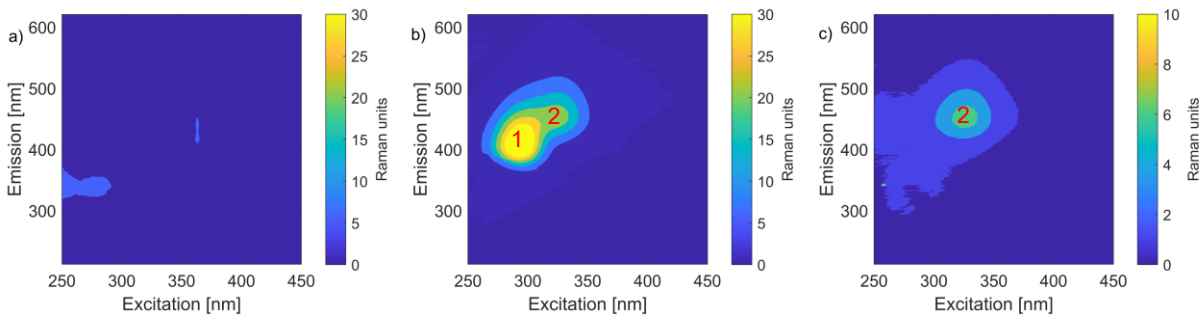

Figure 6: EEMs (a) before UV/H_2O_2 oxidation (0a), (b) after oxidation (1a), and (c) after biodegradation (1a).

To gain further insights into the nature of this recalcitrant organic carbon, we coupled LC-high-resolution mass spectrometry (LC-HRMS) with fluorescence detection. LC-HRMS with fluorescence detection of 290/410 and 320/450 nm revealed that UV/H_2O_2 treatment (sample 1a) caused formation of a wide array of different TPs. Overall, 15 TPs were identified based on signal intensity, and sum formulas were determined using exact masses with a maximal mass error of 5 ppm (Figure 7, Table S11, SI). TP138 could be identified as salicylic acid by retention time comparison with a purchased standard. The TPs 154a, 154b ($C_7H_6O_4$) and 170 ($C_7H_6O_5$) are likely other expected di- and tri-hydroxylated products from BA oxidation. TPs 168, 172a, 172b and 184 were only formed in UV/H2O2 treatment and might represent quinones that are also known intermediates from ozonation of phenol (Ramseier and von Gunten, 2009). Additionally, very polar TPs likely containing a hydroxyl and a sulfate group (TP234a, b, and c with sum formula $C_7H_6O_7S$) were detected that may be products of radical reactions of the aromatic ring with sulfate present in the TW. TPs containing nitrogen as unwanted and potentially toxic side-products could not be identified, but their formation may occur in water with higher nitrite or nitrate concentrations (Rayaroth et al., 2022).

The fluorescence measurement over the whole LC-HRMS method confirmed that the first of the two fluorescence maximum regions (290/410 nm) seen in EEMs of UV/H_2O_2 samples can be linked to salicylic acid (TP138) at RT 5.16 min. This hydroxylated TP is being formed especially during UV/H_2O_2 treatment (as discussed in 3.2.1 for BTE) and is also present in smaller quantities after O_3/H_2O_2 treatment (Figure S16, SI). The fluorescence of peak region 2 (320/450 nm) was visible in all samples in the first 4-5 min of the chromatogram and can generally be assigned to the identified more polar TPs (Figure S14-S17, SI). Interestingly, the fluorescence signal was present even where no peaks were

identified, suggesting that a large number of TPs with low abundance were formed that are not included in this list. The signal was substantially weakened after biodegradation compared to after AOP treatment, but still at much higher intensity than in the control samples without oxidative treatment, before and after biodegradation.

In contrast, a limited number of TPs was detected in the ozonated sample (1b), which is attributed to the reactivity of activated aromatic rings with ozone (Figure 7b). Within the group of identified TPs, only the sulfate-containing TP234a and a trace of TP138 was still found in both samples (1a and 1b) after biodegradation. No dimers or other polymers, that were already reported for ozonation of aniline and phenol, were found in this analysis (Shang and Yu, 2002; Ye and Schuler, 1989). Dimers and polymers were expected to be retained even longer than the parent compound on the reversed-phase column, but no respective mass and fluorescence signals were observed in the relevant time period. Nevertheless, it cannot be excluded that dimers and polymers remained undetected due to ionization problems during MS measurements or the low concentration of isomeric substances in the samples. Furthermore, very polar compounds, such as short-chained organic acids would not be detected in this HPLC-method due to limited retention on the column.

In accordance with DOC data (Figure 5b), BA in samples without oxidation (0a and 0b) was biodegraded completely with almost no detectable TPs after biodegradation. Only weak signals of TP138 in both, and TP166 and TP170 in (0b) could be detected (Figure 7). This confirms that aerobic biodegradation of the parent compound was more complete in this experimental set-up.

The transferability of the results of initial biodegradation to real groundwater contamination scenarios must be evaluated with care: first, the effect of microbial adaptation is not fully taken into account here, thus it is possible that similar biodegradation of oxidized vs. not oxidized samples can be achieved if the microbial community is pre-exposed and adapted. Second, a direct transfer of BA biodegradation to BTE(X) is not possible due to different toxicity thresholds that may inhibit microbiological activity in a fundamentally different way, although past research has shown that certain bacteria strains can handle hundred or more mg L^{-1} BTEX (El-Naas et al., 2014; Wolicka et al., 2009; Xin et al., 2013).

Nevertheless, we conclude that the benefits of AOPs compared to aerobic biological treatment, for instance stimulated by passive oxygen release (Chapman et al., 1997), should be re-assessed for removal of monocyclic aromatics with respect to BA results. This is especially the case for *in-situ* groundwater remediation scenarios with several mg L^{-1} contaminant, where full mineralization by chemical oxidation cannot be guaranteed due to limited process control. For instance, Yang et al. (2020) suggested the use of persulfate or H_2O_2 with Fe^{2+} for *in-situ* oxidation of BTEX. They observed a substantial but not always complete removal of their contaminants in column studies with soil, thus it would be worth looking closer at the remaining dissolved organic compounds. We therefore recommend checking for color and fluorescence increases, which are parameters comparably easy to measure.

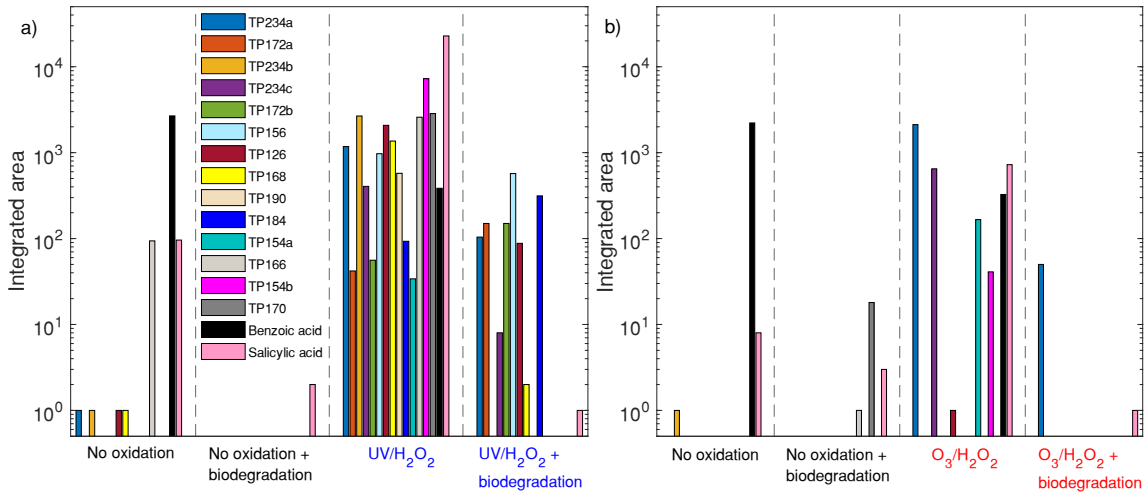

Figure 7: Integrated peak areas of identified TPs, grouped by retention time, before and after biological degradation for samples treated with a) UV/H_2O_2 (sample 1a), and b) O_3/H_2O_2 (sample 1b), and the respective control samples without chemical oxidation (0a and 0b).

4 Conclusions

O_3/H_2O_2 and UV/H_2O_2 AOPs are viable technologies for the oxidation of monocyclic aromatics BTE and BA if removal of target contaminants from treated water is the main objective. DOC removal in both processes was at maximum 20% for removal of BA up to 94%, and multiple organic TPs were formed. The detection of absorbance changes and quantification of hydroxylated TPs in BTE and BA oxidation experiments indicate that some intermediates are oxidized more efficiently during O_3/H_2O_2 treatment. This confirms hypothesized synergies of ozone and $^{\cdot}OH$ exposure in a direct comparison. Nevertheless, absorbance of UV and visible light increased in both treatment processes, where only

partial oxidation was investigated. Additionally, results from biodegradation experiments with BA and TPs provide strong evidence that coupling both AOPs with biological post-treatment is not beneficial for fast, complete mineralization compared to direct biotransformation of the parent compound. Higher oxidant exposures, potentially multiple times higher than needed for removal of parent compounds, are required to achieve a more complete mineralization. Further research is needed to assess the toxicological relevance of the remaining organics, as well as a potential microbial adaptation for improved mineralization of TPs during long-term exposure. In this context, evaluation of field sites with *in-situ* chemical oxidation of BTEX may provide valuable information.

5 Acknowledgement

This study was funded by the German Federal Ministry of Education and Research (BMBF), funding code 02WIL1523. We would like to thank Dr. Oliver Knoop for his help with GC-FID method development and analysis, Kristina Mraz for her help with BTE experiments, Carl Witthöft for his help with biodegradation tests, and Myriam Reif for analyzing TOC/DOC.

6 Declaration of competing interest

The authors declare that they have no known competing financial interests or personal relationships that could have appeared to influence the work reported in this paper.

References

Alapi, T., Dombi, A., 2007. Comparative study of the UV and UV/VUV-induced photolysis of phenol in aqueous solution. Journal of Photochemistry and Photobiology A: Chemistry 188 (2-3), 409–418.

Bahram, M., Bro, R., Stedmon, C., Afkhami, A., 2006. Handling of Rayleigh and Raman scatter for PARAFAC modeling of fluorescence data using interpolation. Journal of Chemometrics 20 (3-4), 99–105.

Bein, E., Zucker, I., Drewes, J.E., Hübner, U., 2021. Ozone membrane contactors for water and wastewater treatment: A critical review on materials selection, mass transfer and process design. Chemical Engineering Journal 413 (18), 127393.

Bustillo-Lecompte, C.F., Kakar, D., Mehrvar, M., 2018. Photochemical treatment of benzene, toluene, ethylbenzene, and xylenes (BTEX) in aqueous solutions using advanced oxidation processes: Towards a cleaner production in the petroleum refining and petrochemical industries. Journal of Cleaner Production 186 (2), 609–617.

Buxton, G.V., Greenstock, C.L., Helman, W.P., Ross, A.B., 1988. Critical Review of rate constants for reactions of hydrated electrons, hydrogen atoms and hydroxyl radicals (·OH/·O − in Aqueous Solution. Journal of Physical and Chemical Reference Data 17 (2), 513–886.

Chapman, S.W., Byerley, B.T., Smyth, D.J.A., Mackay, D.M., 1997. A Pilot Test of Passive Oxygen Release for Enhancement of In-situ Bioremediation of BTEX-Contaminated Ground Water. Groundwater Monitoring & Remediation 17 (2), 93–105.

Chun, H., Yizhong, W., Hongxiao, T., 2000. Destruction of phenol aqueous solution by photocatalysis or direct photolysis. Chemosphere 41 (8), 1205–1209.

Criegee, R., 1975. Mechanismus der Ozonolyse. Angewandte Chemie 87 (21), 765–771.

Cui, H., Gu, X., Lu, S., Fu, X., Zhang, X., Fu, G.Y., Qiu, Z., Sui, Q., 2017. Degradation of ethylbenzene in aqueous solution by sodium percarbonate activated with EDDS–Fe(III) complex. Chemical Engineering Journal 309, 80–88.

Dutschke, M., Schnabel, T., Schütz, F., Springer, C., 2022. Degradation of chlorinated volatile organic compounds from contaminated ground water using a carrier-bound TiO2/UV/O3-system. Journal of environmental management 304, 114236.

El-Naas, M.H., Acio, J.A., El Telib, A.E., 2014. Aerobic biodegradation of BTEX: Progresses and Prospects. Journal of Environmental Chemical Engineering 2 (2), 1104–1122.

Fernandes, A., Gągol, M., Makoś, P., Khan, J.A., Boczkaj, G., 2019a. Integrated photocatalytic advanced oxidation system (TiO_2/UV/O_3/H_2O_2) for degradation of volatile organic compounds. Separation and Purification Technology 224, 1–14.

Fernandes, A., Makoś, P., Khan, J.A., Boczkaj, G., 2019b. Pilot scale degradation study of 16 selected volatile organic compounds by hydroxyl and sulfate radical based advanced oxidation processes. Journal of Cleaner Production 208, 54–64.

Garoma, T., Gurol, M.D., Osibodu, O., Thotakura, L., 2008. Treatment of groundwater contaminated with gasoline components by an ozone/UV process. Chemosphere 73 (5), 825–831.

Hatipoglu, A., Vione, D., Yalçın, Y., Minero, C., Çınar, Z., 2010. Photo-oxidative degradation of toluene in aqueous media by hydroxyl radicals. Journal of Photochemistry and Photobiology A: Chemistry 215 (1), 59–68.

Hoigné, J., Bader, H., 1983. Rate constants of reactions of ozone with organic and inorganic compounds in water—I. Water Research 17 (2), 173–183.

Huang, D., Hu, C., Zeng, G., Cheng, M., Xu, P., Gong, X., Wang, R., Xue, W., 2017. Combination of Fenton processes and biotreatment for wastewater treatment and soil remediation. The Science of the Total Environment 574, 1599–1610.

Huang, X., Li, X., Pan, B., Li, H., Zhang, Y., Xie, B., 2015. Self-enhanced ozonation of benzoic acid at acidic pHs. Water Research 73, 9–16.

Hübner, U., Miehe, U., Jekel, M., 2012. Optimized removal of dissolved organic carbon and trace organic contaminants during combined ozonation and artificial groundwater recharge. Water Research 46 (18), 6059–6068.

Itzel, F., Baetz, N., Hohrenk, L.L., Gehrmann, L., Antakyali, D., Schmidt, T.C., Tuerk, J., 2020. Evaluation of a biological post-treatment after full-scale ozonation at a municipal wastewater treatment plant. Water Research 170, 115316.

Kasprzyk-Hordern, B., Andrzejewski, P., Nawrocki, J., 2005. Catalytic Ozonation of Gasoline Compounds in Model and Natural Water in the Presence of Perfluorinated Alumina Bonded Phases. Ozone: Science & Engineering 27 (4), 301–310.

Katsoyiannis, I.A., Canonica, S., Gunten, U. von, 2011. Efficiency and energy requirements for the transformation of organic micropollutants by ozone, O_3/H_2O_2 and UV/H_2O_2. Water Research 45 (13), 3811–3822.

Krembs, F.J., Siegrist, R.L., Crimi, M.L., Furrer, R.F., Petri, B.G., 2010. ISCO for Groundwater Remediation: Analysis of Field Applications and Performance. Groundwater Monitoring & Remediation 30 (4), 42–53.

Lamsal, R., Walsh, M.E., Gagnon, G.A., 2011. Comparison of advanced oxidation processes for the removal of natural organic matter. Water Research 45 (10), 3263–3269.

Leiknes, T., Phattaranawik, J., Boller, M., von Gunten, U., Pronk, W., 2005. Ozone transfer and design concepts for NOM decolourization in tubular membrane contactor. Chemical Engineering Journal 111 (1), 53–61.

Merényi, G., Lind, J., Naumov, S., von Sonntag, C., 2010. The reaction of ozone with the hydroxide ion: mechanistic considerations based on thermokinetic and quantum chemical calculations and the role of HO4- in superoxide dismutation. Chemistry - A European Journal 16 (4), 1372–1377.

Miklos, D.B., Hartl, R., Michel, P., Linden, K.G., Drewes, J.E., Hübner, U., 2018. UV/H_2O_2 process stability and pilot-scale validation for trace organic chemical removal from wastewater treatment plant effluents. Water Research 136, 169–179.

Miklos, D.B., Wang, W.-L., Linden, K.G., Drewes, J.E., Hübner, U., 2019. Comparison of UV-AOPs (UV/H_2O_2, UV/PDS and UV/Chlorine) for TOrC removal from municipal wastewater effluent and optical surrogate model evaluation. Chemical Engineering Journal 362, 537–547.

Müller, J., Drewes, J.E., Hübner, U., 2017. Sequential biofiltration - A novel approach for enhanced biological removal of trace organic chemicals from wastewater treatment plant effluent. Water Research 127, 127–138.

Mvula, E., von Sonntag, C., 2003. Ozonolysis of phenols in aqueous solution. Organic & Biomolecular Chemistry 1 (10), 1749–1756.

Nagakura, S., Kuboyama, A., 1954. Dipole Moments and Absorption Spectra of o-Benzoquinone and its Related Substances. Journal of the American Chemical Society 76 (4), 1003–1005.

Ni, Y., Su, S., Kokot, S., 2006. Spectrofluorimetric studies on the binding of salicylic acid to bovine serum albumin using warfarin and ibuprofen as site markers with the aid of parallel factor analysis. Analytica chimica acta 580 (2), 206–215.

Nimmer, M.A., Wayner, B.D., Allen Morr, A., 2000. In-situ ozonation of contaminated groundwater. Environmental Progress 19 (3), 183–196.

Nöthe, T., Fahlenkamp, H., von Sonntag, C., 2009. Ozonation of wastewater: rate of ozone consumption and hydroxyl radical yield. Environmental Science & Technology 43 (15), 5990–5995.

Oller, I., Malato, S., Sánchez-Pérez, J.A., 2011. Combination of Advanced Oxidation Processes and biological treatments for wastewater decontamination—A review. Science of The Total Environment 409 (20), 4141–4166.

Pariente, M., Martinez, F., Melero, J., Botas, J., Velegraki, T., Xekoukoulotakis, N., Mantzavinos, D., 2008. Heterogeneous photo-Fenton oxidation of benzoic acid in water: Effect of operating

conditions, reaction by-products and coupling with biological treatment. Applied Catalysis B: Environmental 85 (1-2), 24–32.

Park, H., Choi, W., 2005. Photocatalytic conversion of benzene to phenol using modified TiO2 and polyoxometalates. Catalysis Today 101 (3-4), 291–297.

Ramseier, M.K., von Gunten, U., 2009. Mechanisms of Phenol Ozonation—Kinetics of Formation of Primary and Secondary Reaction Products. Ozone: Science & Engineering 31 (3), 201–215.

Rayaroth, M.P., Aravindakumar, C.T., Shah, N.S., Boczkaj, G., 2022. Advanced oxidation processes (AOPs) based wastewater treatment - unexpected nitration side reactions - a serious environmental issue: A review. Chemical Engineering Journal 430 (3), 133002.

Rayaroth, M.P., Marchel, M., Boczkaj, G., 2023. Advanced oxidation processes for the removal of mono and polycyclic aromatic hydrocarbons - A review. The Science of the Total Environment 857 (Pt 2), 159043.

Real, F.J., Benitez, F.J., Acero, J.L., Sagasti, J.J.P., Casas, F., 2009. Kinetics of the Chemical Oxidation of the Pharmaceuticals Primidone, Ketoprofen, and Diatrizoate in Ultrapure and Natural Waters. Industrial & Engineering Chemistry Research 48 (7), 3380–3388.

Rosenfeldt, E.J., Linden, K.G., Canonica, S., Gunten, U. von, 2006. Comparison of the efficiency of *OH radical formation during ozonation and the advanced oxidation processes O_3/H_2O_2 and UV/H_2O_2. Water Research 40 (20), 3695–3704.

Schollée, J.E., Bourgin, M., Gunten, U. von, McArdell, C.S., Hollender, J., 2018. Non-target screening to trace ozonation transformation products in a wastewater treatment train including different post-treatments. Water Research 142, 267–278.

Schuler, R.H., Albarran, G., 2002. The rate constants for reaction of OH radicals with benzene and toluene. Radiation Physics and Chemistry 64 (3), 189–195.

Seiwert, B., Nihemaiti, M., Bauer, C., Muschket, M., Sauter, D., Gnirss, R., Reemtsma, T., 2021. Ozonation products from trace organic chemicals in municipal wastewater and from metformin: peering through the keyhole with supercritical fluid chromatography-mass spectrometry. Water Research 196, 117024.

Sgroi, M., Anumol, T., Vagliasindi, F.G.A., Snyder, S.A., Roccaro, P., 2021. Comparison of the new Cl2/O3/UV process with different ozone- and UV-based AOPs for wastewater treatment at pilot scale: Removal of pharmaceuticals and changes in fluorescing organic matter. The Science of the Total Environment 765, 142720.

Shang, N.C., Yu, Y.H., 2002. Toxicity and color formation during ozonation of mono-substituted aromatic compounds. Environmental technology 23 (1), 43–52.

Siegrist, R.L., Crimi, M., Simpkin, T.J., 2011. In-situ Chemical Oxidation for Groundwater Remediation. SERDP/ESTCP Environmental Remediation Technology 3. Springer Science+Business Media LLC, New York, NY.

Sutton, N.B., Grotenhuis, J.T.C., Langenhoff, A.A.M., Rijnaarts, H.H.M., 2011. Efforts to improve coupled in-situ chemical oxidation with bioremediation: a review of optimization strategies. Journal of Soils and Sediments 11 (1), 129–140.

von Sonntag, C., von Gunten, U., 2012. Chemistry of ozone in water and wastewater treatment: From basic principles to applications. IWA Publishing, London.

Wenk, J., Aeschbacher, M., Salhi, E., Canonica, S., Gunten, U. von, Sander, M., 2013. Chemical oxidation of dissolved organic matter by chlorine dioxide, chlorine, and ozone: effects on its optical and antioxidant properties. Environmental Science & Technology 47 (19), 11147–11156.

Wolicka, D., Suszek, A., Borkowski, A., Bielecka, A., 2009. Application of aerobic microorganisms in bioremediation in-situ of soil contaminated by petroleum products. Bioresource technology 100 (13), 3221–3227.

Wünsch, R., Mayer, C., Plattner, J., Eugster, F., Wülser, R., Gebhardt, J., Hübner, U., Canonica, S., Wintgens, T., Gunten, U. von, 2021. Micropollutants as internal probe compounds to assess UV fluence and hydroxyl radical exposure in UV/H_2O_2 treatment. Water Research 195, 116940.

Xin, B.-P., Wu, C.-H., Wu, C.-H., Lin, C.-W., 2013. Bioaugmented remediation of high concentration BTEX-contaminated groundwater by permeable reactive barrier with immobilized bead. Journal of Hazardous Materials 244-245, 765–772.

Yang, Z.-H., Verpoort, F., Dong, C.-D., Chen, C.-W., Chen, S., Kao, C.-M., 2020. Remediation of petroleum-hydrocarbon contaminated groundwater using optimized in-situ chemical oxidation system: Batch and column studies. Process Safety and Environmental Protection 138 (Part B), 18–26.

Ye, M., Schuler, R.H., 1989. Second-order combination reactions of phenoxyl radicals. The Journal of Physical Chemistry 93 (5), 1898–1902.

Zhang, Y., Li, K., Wang, J., Hou, D., Liu, H., 2017. Ozone mass transfer behaviors on physical and chemical absorption for hollow fiber membrane contactors. Water Science & Technology 76 (5-6), 1360–1369.